

## Light Nuclei Emitted in the Fission of $^{252}\text{Cf}\dagger$

G. M. RAISBECK AND T. D. THOMAS\*

*Frick Chemical Laboratory and Princeton-Pennsylvania Accelerator,  
Princeton University, Princeton, New Jersey*

(Received 19 February 1968)

Energy spectra and angular distributions have been measured for  $^1\text{H}$ ,  $^2\text{H}$ ,  $^3\text{H}$ ,  $^4\text{He}$ ,  $^6\text{He}$ ,  $^8\text{He}$ ,  $\text{Li}$ , and  $\text{Be}$  ions emitted in coincidence with the spontaneous fission of  $^{252}\text{Cf}$ . The data show that, with the possible exception of  $^1\text{H}$ , all of the particles are strongly peaked at  $90^\circ$  with respect to the major fragments, and are probably released by a common mechanism. Using a point-charge model, with various combinations of starting conditions, we have made trajectory calculations for each type of particle. It was found that reasonable agreement with the measured results could be obtained by using a consistent set of initial conditions: namely, a release time of  $0.4 \times 10^{-21}$  sec, corresponding to a separation distance of  $21.5 \times 10^{-18}$  cm for the major fragments, and an average initial energy of 2 MeV for the third particle. Both the angular distribution and the energy spectra of the  $^1\text{H}$  particles appear to be somewhat anomalous in comparison with the calculations, and several possible reasons for this are discussed. We have also observed for the first time isotopes of boron and carbon from the fission of  $^{252}\text{Cf}$ , and give limits on the energy and yield of heavier particles.

### I. INTRODUCTION

IT has been known for some time that, once in every several hundred fission events, the normal binary fragments are accompanied by an additional light charged particle.<sup>1</sup> It has been noted that, because of the conditions under which such particles are emitted, they may give significant information about the fission process itself, and of nuclear matter in general.<sup>2</sup>

The preponderance of light fragments are  $\alpha$  particles, with an energy distribution peaked at about 15 MeV, and an angular distribution strongly peaked at about  $90^\circ$  with respect to the large fragments. This latter characteristic has been taken as evidence that they are formed between the fragments, near the time of scission.<sup>3</sup> Except for the expected loss of mass and kinetic energy by the larger fragments, these so-called "long-range  $\alpha$ " events appear to be very representative of normal binary fission.<sup>4,5</sup> A review of the literature on long-range  $\alpha$  particles and on protons and tritons believed to be associated with fission is given by Hyde.<sup>6</sup>

More recently, improved counter techniques have permitted a more thorough study of such particles. Fraenkel has made a very detailed analysis of the distribution of long-range  $\alpha$  particles and their correlation with various mass and energy divisions in fission.<sup>5</sup> Also, heavier particles, including  $^6\text{He}$ ,  $^8\text{He}$ , and isotopes of lithium and beryllium emitted from spontaneously

fissioning  $^{252}\text{Cf}$  have been reported by Thomas and Whetstone,<sup>7,8</sup> and by Cospers, Cerny, and Gatti.<sup>9</sup>

Although all these particles have generally been assumed to be released in coincidence with the fission process, there has been no experimental verification that this is so except in the case of  $^4\text{He}$ . The present studies were undertaken to confirm this point, and to investigate the energy and angular distributions of the coincident particles. In addition, we have attempted to make a consistent set of calculations, based on a model suggested by Halpern,<sup>2</sup> by which the basic features of such distributions can be understood.

During the course of these experiments we have also observed for the first time the emission of boron and carbon isotopes from  $^{252}\text{Cf}$ , and have obtained limits on the abundance and energy of heavier particles.

### II. EXPERIMENTAL PROCEDURE

A schematic drawing of the experimental apparatus is shown in Fig. 1. The  $^{252}\text{Cf}$  source, which had an

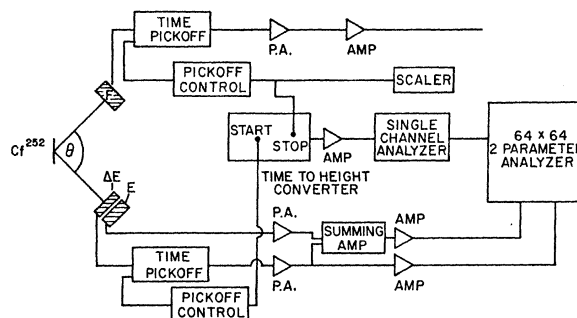


Fig. 1. Schematic diagram of the experimental setup.

<sup>7</sup> S. L. Whetstone, Jr., and T. D. Thomas, *Phys. Rev. Letters* **15**, 298 (1965).

<sup>8</sup> S. L. Whetstone, Jr., and T. D. Thomas, *Phys. Rev.* **154**, 1174 (1967).

<sup>9</sup> S. W. Cospers, J. Cerny, and R. G. Gatti, *Phys. Rev.* **154**, 1193 (1967).

<sup>†</sup> Supported in part by the U. S. Atomic Energy Commission.

\* Alfred P. Sloan Fellow.

<sup>1</sup> A summary of the early work is given by W. J. Whitehouse, *Progress in Nuclear Physics* (Academic Press Inc., New York, 1952), Vol. 2, pp. 158-163.

<sup>2</sup> I. Halpern, CERN Report No. CERN-6812, 1963 (unpublished); *Physics and Chemistry of Fission* (International Atomic Energy Agency, Vienna, 1965), Vol. II, p. 369.

<sup>3</sup> Tsien San-Tsiang, *J. Phys. Radium* **9**, 6 (1948).

<sup>4</sup> H. Schmitt, J. Neiler, F. Walter, and A. Chetham-Strode, *Phys. Rev. Letters* **9**, 427 (1962).

<sup>5</sup> Z. Fraenkel, *Phys. Rev.* **156**, 1283 (1967).

<sup>6</sup> E. K. Hyde, *The Nuclear Properties of the Heavy Elements* (Prentice-Hall Publishers, Inc., Englewood Cliffs, N. J., 1964), Vol. III, pp. 131-140.

intensity of  $4 \times 10^7$  fissions/min, was prepared by self-transfer from a larger source onto a thin nickel foil. This foil was then placed on a thick aluminum backing, and a cover foil of  $450 \mu\text{g}/\text{cm}^2$  of nickel was placed over the  $^{252}\text{Cf}$  to prevent contamination of the chamber.

Identification of the light particles was accomplished by a simple two-counter telescope that recorded  $\Delta E$  and  $E$  of each event. The  $E$  detector was a lithium-drifted silicon device with a thickness of 2 mm. For most of the work the  $\Delta E$  detector was a surface-barrier type, having a totally depleted thickness of  $62 \mu$ . For the heavier particles a diffused-junction detector of either 12 or  $14 \mu$  was used. The  $\Delta E$  detector was 3.5 cm from the source, and collimators restricted the acceptance angle of the telescope system to about  $7^\circ$ . The collimating system also contained an aluminum foil of sufficient thickness to prevent the natural  $\alpha$  particles and fission fragments from reaching the detectors. In most cases this was  $9.35 \text{ mg}/\text{cm}^2$ , while for the heavier particles it was  $7.6 \text{ mg}/\text{cm}^2$ .

Fission fragments were detected with ORTEC heavy-ion surface-barrier detectors. Because of the very high fission counting rate ( $\sim 10^6$  counts/min), these detectors deteriorated rapidly, and the bias voltage had to be periodically adjusted to compensate for the increasing leakage current. It was found that these detectors could be used satisfactorily for a total exposure of approximately  $3 \times 10^9$  fission fragments, at which time they had a leakage current of about  $100 \mu\text{A}$ . Although the spectral qualities were severely deteriorated before this, the timing signal was not significantly affected. The fission detector was collimated to an acceptance angle of  $20^\circ$ , or in a few runs,  $30^\circ$ .

The pulses from the  $\Delta E$  and fission detectors initially passed through time pick-off units, which generated start and stop signals, respectively, for a time-to-pulse-height converter (THC). The output of the THC was fed to a single-channel analyzer. When the single-channel analyzer indicated that the start and stop signals had the time relationship characteristic of a true coincidence, a gating signal was sent to a two-parameter analyzer. A 30-nsec resolution time was used, with a typical timing spectrum giving a peak of 5 nsec full width at half-maximum (FWHM). The chance coincidence rate under these conditions was negligible.

After normal amplification the  $\Delta E$  signal and the sum of  $\Delta E + E$  were stored in the  $64 \times 64$  matrix of the analyzer. The display from such a system and the method of identification have been previously discussed.<sup>8</sup> An energy calibration of the detectors was obtained using the  $\alpha$  particles from an  $^{241}\text{Am}$  standard and a pulser. Stability checks were made on the system periodically using the pulser.

In an attempt to look at the lowest-energy heavy particles, several noncoincidence runs were made in which the aluminum foil in front of the counter telescope was reduced to  $4.7 \text{ mg}/\text{cm}^2$ . In these cases the natural

$\alpha$  particles penetrated into the  $\Delta E$  detector (but not the  $E$ ), depositing about 2.5 MeV. Gating signals were taken from the  $E$  detector in order to minimize analyzer dead time. The pileup rate in this mode was about 5%, so it was restricted only to particles heavier than lithium.

### III. RESULTS

Our coincidence results confirm that all the light particles previously associated with the spontaneous fission of  $^{252}\text{Cf}$  do indeed occur during the fission process. In addition, with the possible exception of  $^1\text{H}$ , they all appear to exhibit the same strong angular correlation at about  $90^\circ$  with respect to the large fragments, thus suggesting that they are formed in the neck region at, or shortly after, the time of scission.

The angular distributions for  $^3\text{H}$ ,  $^4\text{He}$ , and  $^6\text{He}$  are given in Fig. 2. They may be adequately described by the solid curves, which are Gaussian distributions that have been broadened by an amount appropriate to allow for the finite detector resolution. The peak positions are slightly greater than  $90^\circ$ , as dictated by

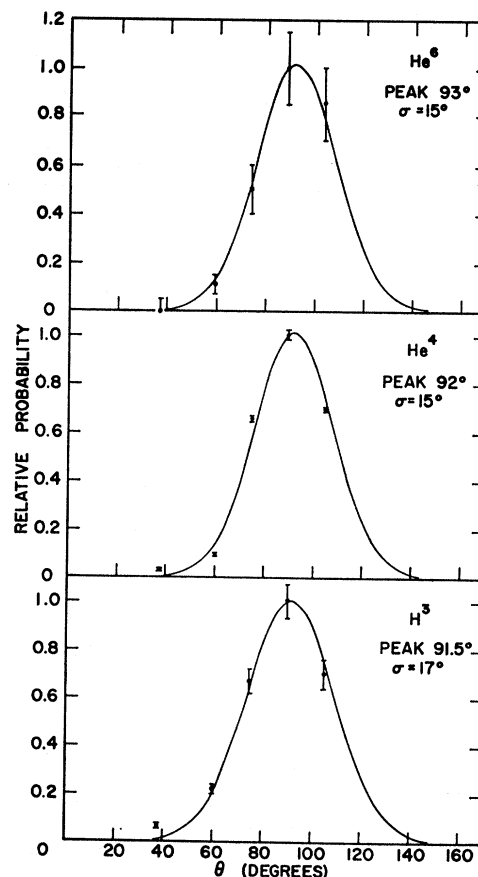


FIG. 2. Angular distribution of  $^3\text{H}$ ,  $^4\text{He}$ , and  $^6\text{He}$  with respect to the fission fragments (all masses). The solid curves are Gaussian distributions having the variances indicated and broadened to correct for the finite detector resolution.

the recoil momentum of the emitted particle. The errors indicated are statistical, based on the counting rates only. The distributions are very similar, although that of  $^3\text{H}$  is apparently slightly broader than that of  $^4\text{He}$ .

The angular distribution for  $^4\text{He}$  measured here is in good agreement with those given by Atneosen, Thomas, and Garvey and by Thomas and Whetstone,<sup>10</sup> but is significantly narrower than that given by Fraenkel.<sup>5</sup> He has measured the distribution of long-range  $\alpha$  particles with respect to the light-mass fission fragment only, and reports a FWHM of  $32^\circ$ . If the complementary distribution with respect to the heavy fragment is folded in, an over-all FWHM of  $49^\circ$  is obtained, as compared with  $35^\circ$  from our work.

Because of the low abundance of the heavier particles, the full angular distributions were not measured. However, the limited data on  $^8\text{He}$ , lithium, and beryllium ions give a  $90^\circ/60^\circ$  ratio of greater than 8, thus indicating that these particles also are strongly peaked.

The situation for  $^1\text{H}$  is somewhat less clear. The abundance of coincident protons is low; the coincident counting rate was less than 1 per h. As indicated in Fig. 3, the protons appear to occur with a much broader angular distribution than the other "scission" particles. As will be shown later, the proton energy spectrum is also somewhat anomalous.

The statistics on the even less abundant  $^2\text{H}$  (Fig. 3) particles are poor, but suggest a moderate peaking, somewhere intermediate between  $^1\text{H}$  and  $^3\text{H}$ .

In Fig. 4 the energy spectra for  $^1\text{H}$ ,  $^3\text{H}$ , and  $^4\text{He}$  at

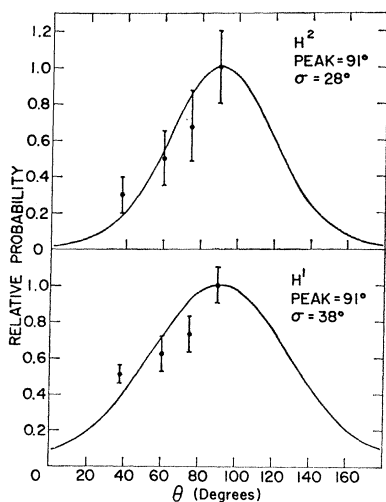


FIG. 3. Angular distribution of  $^1\text{H}$  and  $^2\text{H}$  with respect to the fission fragments (all masses). The solid curves are Gaussian distributions having the variances indicated and broadened to correct for the finite detector resolution. The fit to the measured points in these cases is approximate and is given primarily for comparison purposes.

<sup>10</sup> R. A. Atneosen, T. D. Thomas, and G. T. Garvey, Phys. Rev. **139**, B307 (1965); T. D. Thomas and S. L. Whetstone, Jr., *ibid.* **144**, 1060 (1966).

various angles are shown, together with the noncoincident spectra. The characteristics of the  $^3\text{H}$  and  $^4\text{He}$  distributions are very similar. Initially, as one moves away from  $90^\circ$ , the dispersion of the distribution increases, and then the peak position gradually increases to higher energies. The same general trend was observed for  $^2\text{H}$  and  $^6\text{He}$ , although the statistics are very limited. This correlation of higher energies with a wider angular distribution, first pointed out by Perfilov,<sup>11</sup> has been measured for  $^4\text{He}$  from  $^{252}\text{Cf}$  by Fraenkel,<sup>5</sup> but he has reported a much weaker correlation than we have observed.

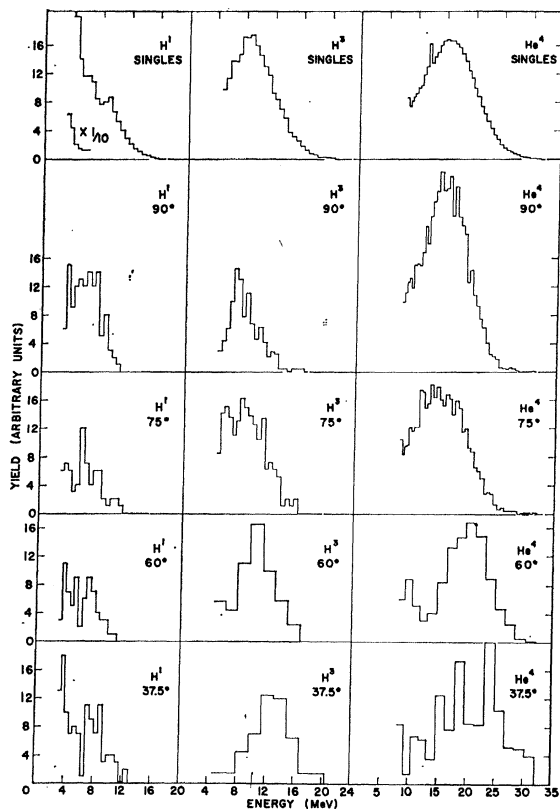


FIG. 4. Energy spectra for  $^1\text{H}$ ,  $^3\text{H}$ , and  $^4\text{He}$  measured at various angles with respect to the fission fragments. At the top the singles spectra are shown.

The most notable characteristic of the  $^1\text{H}$  result is the fact that a large number of low-energy protons ( $<6$  MeV) of the singles spectra are not observed in coincidence at any of the angles measured. Such events are presumably the result of scattering or secondary reactions, as has been indicated by Cospers, Cerny, and Gatti.<sup>9</sup> The shape of the coincident proton spectra in Fig. 4 remains somewhat uncertain because of the poor counting statistics. There does seem to be some indica-

<sup>11</sup> N. Perfilov and Z. Solov'eva, Zh. Eksperim. i Teor. Fiz. **37**, 1157 (1959) [English transl.: Soviet Phys.—JETP **10**, 824 (1960)].

tion that the highest-energy events are associated with the smaller angles. However, the bulk of the  $^1\text{H}$  spectrum appears to be rather insensitive to angle.

We have also made a number of long runs without any coincidence requirement in order to look at the over-all energy spectra of lithium and beryllium ions. During this time we have observed over 100 events identifiable as boron and carbon ions. An example of some of these events is given in Fig. 5. Although Cosper, Cerny, and Gatti looked for, and reported, the absence of such particles,<sup>9</sup> our setup was such that the lower-energy cutoff was slightly below theirs.

In an attempt to lower this cutoff further, we reduced the aluminum foil in front of the counter telescope to

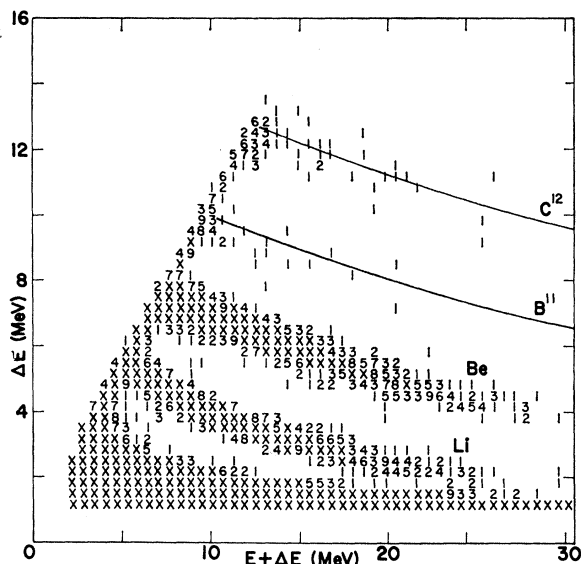


FIG. 5. Example of the  $\Delta E \times (E + \Delta E)$  analyzer output for heavy isotopes emitted in the spontaneous fission of  $^{252}\text{Cf}$ . The foil in front of the counter telescope was  $7.61 \text{ mg/cm}^2$  of aluminum, and the energies shown are those actually deposited in the detectors. The thickness of the  $\Delta E$  detector was  $12 \mu$ . Crosses indicate channels having more than nine events, and the solid lines are the calculated loci for  $^{11}\text{B}$  and  $^{12}\text{C}$  ions.

$4.7 \text{ mg/cm}^2$ . The pileup rate ( $\sim 5\%$ ) in this mode restricted its applicability (natural  $\alpha$  particles plus long-range  $\alpha$  particles or beryllium can simulate lithium- or boron-type events, respectively). However, we were able to observe a greatly increased yield of carbon ions at the lower energies. A coincident run was also made with the thin foil, using the  $E$  signal for zero-crossover timing, and a time resolution of  $0.5 \mu\text{sec}$ . A total of seven carbon and four boron events were recorded, while a chance run of the same interval gave one carbon event. We therefore feel fairly confident that these heavier particles do arise from the fission process.

The observable energy spectra for lithium, beryllium, and carbon are shown in Fig. 6. It may be noted that

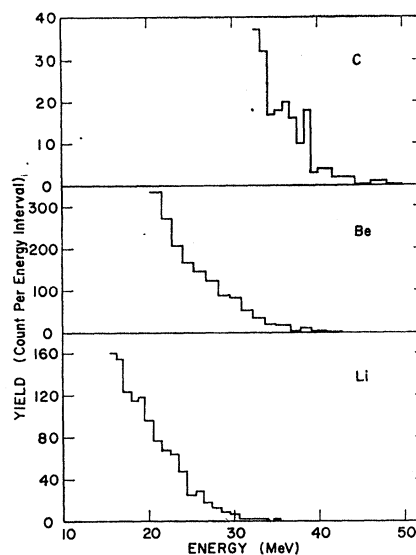


FIG. 6. Observed energy spectra of lithium, beryllium, and carbon isotopes emitted in the spontaneous fission of  $^{252}\text{Cf}$ .

there are no apparent peaks for lithium and beryllium, even though the minimum energies are below the peak positions given by Cosper, Cerny, and Gatti.<sup>9</sup> The reason for this discrepancy is not known, especially since our yields for these particles are in good agreement with theirs.

The yields, over the energy range observed, are given in Table I for each of the particles studied. The  $^1\text{H}$  abundance has been obtained by assuming the angular distribution shown in Fig. 3 and integrating over  $4\pi$  sr. Only the spectrum for  $^4\text{He}$  has been extrapolated to zero energy, and the value of  $3.20 \times 10^{-3}$  per fission is in good agreement with previous work.

In a search for particles with  $Z > 6$ , we made extended runs with both the regular and the reduced foil. The former produced exceptionally clean experiments, with

TABLE I. Abundance of light nuclei observed in the spontaneous fission of  $^{252}\text{Cf}$ .

Particle	Energy range (MeV)	Abundance (per fission)
$^1\text{H}$	3.3-12	$4.6 \pm 0.5 \times 10^{-5}$ <sup>a</sup>
$^2\text{H}$	4.2-18	$1.5 \pm 0.2 \times 10^{-5}$
$^3\text{H}$	5.0-24	$1.98 \pm 0.1 \times 10^{-4}$
$^4\text{He}$	7.1-41	$3.03 \pm 0.1 \times 10^{-3}$ <sup>b</sup>
$^6\text{He}$	14.6-43	$2.9 \pm 0.2 \times 10^{-5}$
$^8\text{He}$	9.6-46	$1.9 \pm 0.3 \times 10^{-6}$
Li	15.7-65	$3.7 \pm 0.2 \times 10^{-6}$
Be	24.1-73	$4.8 \pm 0.2 \times 10^{-6}$
	20.5-70 <sup>c</sup>	$9.1 \pm 0.3 \times 10^{-6}$
B	31.0-75	$0.9 \pm 0.4 \times 10^{-7}$
	25.3-72 <sup>c</sup>	$0.7 \pm 0.2 \times 10^{-6}$ <sup>d</sup>
C	40.5-78	$1.3 \pm 0.4 \times 10^{-7}$
	33.2-75 <sup>c</sup>	$1.4 \pm 0.2 \times 10^{-6}$

<sup>a</sup> Assuming the solid curve shown in Fig. 3.

<sup>b</sup> Extrapolated to zero energy, the  $^4\text{He}$  abundance is  $3.20 \pm 0.1 \times 10^{-3}$ .

<sup>c</sup> Telescope foil reduced to  $4.7 \text{ mg/cm}^2$ .

<sup>d</sup> This is an upper limit because natural  $\alpha$ -particle pileup (5%) on beryllium can give rise to B-type events.

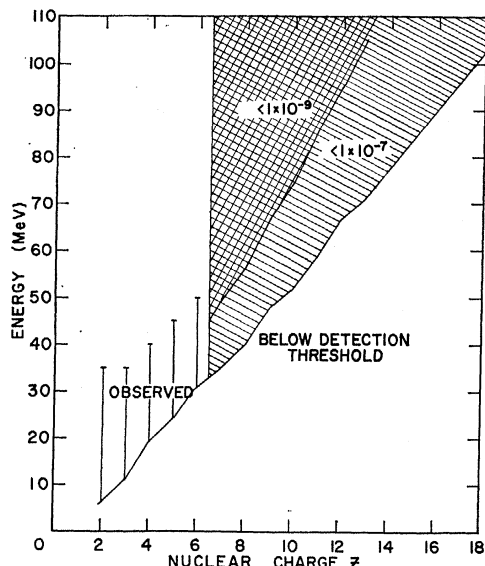


FIG. 7. Upper limits established on the abundances of light nuclei having  $Z > 6$ . Energy limits were established by requiring that any ion traverse the aluminum foil (7.6 or 4.7 mg/cm<sup>2</sup>, respectively) and deposit sufficient energy in the  $\Delta E$  detector to distinguish it from carbon ions.

not a single event above carbon observed in over 10 days of running time. Because of the natural  $\alpha$  particles penetrating the  $\Delta E$  counter, the runs with the thin foil had a background that was significantly higher. In several instances there appeared to be a clustering of events around the positions expected for nitrogen and oxygen ions. However, these were very near the low-energy cutoff, and could not be reliably extracted from the background. The upper limits established by both modes are presented in Fig. 7. These limits are not inconsistent with recent estimates of long-range fragments by Natowitz *et al.*,<sup>12</sup> based on track registration experiments in Lexan and mica. They report substantially higher abundances of carbon, nitrogen, and oxygen than we have seen in our experiments. This apparent discrepancy arises presumably because their system has an effectively lower detection threshold than does ours.

#### IV. THEORETICAL CALCULATIONS

##### Model

The model used to help interpret the experimental results is one suggested by Halpern.<sup>2</sup> We assume that two fission fragments are formed at some time zero and start moving apart under their mutual repulsion. At some time later,  $t$ , a third particle appears at a specified point more or less between the two major fragments and with a specified velocity. The equations of motion are numerically integrated to give the final

velocity (magnitude and direction) of the third particle. The results of a suitable set of such calculations are averaged over an assumed distribution of starting conditions to give energy spectra and angular distributions of the third particles. A comparison of these calculated results with the experimental results allows us to find a set of initial parameters that will give final distributions consistent with experimental results.

The calculations are carried out as if the particles involved were classical point charges. The use of a classical model is dictated by practicality; the alternative is to solve the time-dependent Schrödinger equation in three dimensions. It is felt that the classical calculation should reproduce the major features of the process. Halpern has estimated the error due to treating the particles as points and has concluded that it can be neglected.<sup>2</sup>

For such a three-body calculation there are, in principle, 19 parameters: nine spatial, nine velocity, and  $t$ . Specifying the location of the center of mass and the orientation of the line determined by the two major fragments reduces the number of spatial coordinates to four. Specifying that the center of mass is stationary and that there is no orbital angular momentum between the two major fragments reduces the number of momentum coordinates to four.

We reduce this number further by assuming (1) that the velocity of the two major fragments is zero at time zero and (2) that the third fragment is born on the line joining the two major fragments. The first of these seems reasonable. As to the second, calculations by Halpern<sup>2</sup> and by Boneh, Fraenkel, and Nebenzahl<sup>13</sup> indicate that the final energy of the particle depends only weakly on the initial distance from the axis (unless the third particle is released with zero kinetic energy).

There remain five parameters to be specified. We have chosen to use the following set:

- (1) Time  $t$  at which the third particle is released. The natural time unit for these calculations is  $10^{-21}$  sec.
- (2) The distance between the two fragments at time zero. The value of this parameter determines, to a large extent, the final energy of the fission fragments. A value of  $20.5 \times 10^{-12}$  cm gives reasonable agreement with experiment. This value was used in these calculations.
- (3) The position of the third fragment along the axis of the two major fragments at time  $t$ .
- (4) The kinetic energy of the third fragment at time  $t$ .
- (5) The direction of motion of the third particle relative to the axis at time  $t$ .

The last three are identical to parameters used by Boneh, Fraenkel, and Nebenzahl.<sup>13</sup> The first two are equivalent to their choice of velocity of the heavy

<sup>12</sup> J. B. Natowitz, A. Khodai-Joopari, J. M. Alexander, and T. D. Thomas Phys. Rev. **169**, 993 (1968).

<sup>13</sup> Y. Boneh, Z. Fraenkel, and I. Nebenzahl, Phys. Rev. **156**, 1305 (1967).

fragment and major fragment separation at time  $t$ . There is a unique correspondence between our parameters and theirs.

In addition, it is necessary to specify the charge and mass of the initial fragments. For most of the calculations we have used  $Z=42$  and  $A=108$  for one fragment and  $Z=56$  and  $A=144$  for the other, corresponding approximately to the most probable fragments from  $^{252}\text{Cf}$ . The following assumptions about the distributions of initial conditions were made:

(1) The distribution of release times of the third particle is a  $\delta$  function. We considered a unique time for each case.

(2) The three momentum components of the third particle are Gaussianly distributed about zero with the same standard deviation for each component. This assumption corresponds to an isotropic initial angular distribution. It corresponds to an initial energy distribution  $P(E_0)$ ,

$$P(E_0) \propto E_0^{1/2} \exp[-(3E_0/2\bar{E}_0)],$$

where  $E_0$  is the initial kinetic energy of the particle and  $\bar{E}_0$  is the average initial kinetic energy. The width parameter of momentum distributions is uniquely specified by  $\bar{E}_0$ . The most probable initial energy according to this expression is one-third of the average.

(3) The initial position of the third particle along the interfragment axis was taken to be Gaussian. The most probable position was the point of minimum potential between the two major fragments. We assumed no correlation between the initial position and initial energy, in contrast to Boneh, Fraenkel, and Nebenzahl,<sup>13</sup> who concluded that it was necessary to assume a dependence of the initial kinetic energy on position.

(4) As indicated above, we usually considered only the most probable mass division (although some calculations were done with other divisions in order to observe their effect).

Given these assumptions, it is necessary to specify only three parameters to determine the final angular and energy distribution. These are (1) the release time, (2) the average initial energy, and (3) the width of the Gaussian distribution characterizing the initial position.

#### Method of Calculation

There are nine coupled second-order differential equations to be solved, each of the form

$$M_i \ddot{X}_{ij} = F_{ij},$$

where  $M_i$  is the mass of the  $i$ th particle,  $X_{ij}$  is the  $j$ th spatial coordinate of the  $i$ th particle, and  $F_{ij}$  is the  $j$ th component of the force on the  $i$ th particle. Since all of the forces are Coulomb forces between point charges, the various  $F$ 's can be easily expressed in terms of the coordinates of the three particles. The second-order equations are readily converted to pairs of first-order

equations:

$$M_i \frac{dV_{ij}}{dt} = F_{ij} \quad \text{and} \quad \frac{dX_{ij}}{dt} = V_{ij},$$

where  $V_{ij}$  is the  $j$ th component of the velocity of the  $i$ th particle.

The 18 equations so obtained were integrated numerically on an IBM-7094 computer using a subroutine that automatically chose integration steps of appropriate length. The integrations were continued out to a time of  $100 \times 10^{-21}$  sec, by which time the potential energy had fallen to about 1% of its original value. At the end of the calculation the energy of each of the three fragments and the angles between their directions of motion were calculated.

At the release time  $t$ , the mass and momentum given to the third particle was subtracted from the mass and momentum of the two original particles, so that the total momentum of the system was zero. In general, however, some angular momentum and energy were created with the third particle.

The program was tested in various ways. The momentum at the end of the calculation was found to be zero. The total energy at the end was found to be equal to the total energy at time  $t$ . Results of integrations in which no third particle was released agreed with those that can be easily calculated exactly. Similarly, results obtained for three particles of equal charge and mass and zero velocity released at the corners of an equilateral triangle agreed with those that can be readily determined from the symmetry of the problem. In addition, we repeated several of the calculations reported by Boneh, Fraenkel, and Nebenzahl<sup>13</sup> and obtained good agreement with their results.

Averaging of the calculated trajectories over the assumed initial distribution was done by the Monte Carlo method. Since each trajectory calculation took about 10 sec and it was desirable to consider about 10 000 events for each Monte Carlo calculation, it was necessary to separate the two parts. We found that rather simple empirical formulas could be used to fit the results of the trajectory calculations with good accuracy over the range of the parameters involved.

#### Results of Trajectory Calculations

The dependence of final energy and angle on the initial conditions has been presented by Boneh, Fraenkel, and Nebenzahl.<sup>13</sup> We review them here. Figure 8 shows the final kinetic energy of  $\alpha$  particles,  $E_f$ , as a function of initial energy  $E_0$  and release time. The points represent the results of calculations and the curves empirical fits using the expression

$$E_f = E_0 + A[1 - 1/(1 + B\sqrt{E_0})], \quad (1)$$

where  $A$  and  $B$  are empirical parameters that depend on  $t$ , on the position at which the third particle is

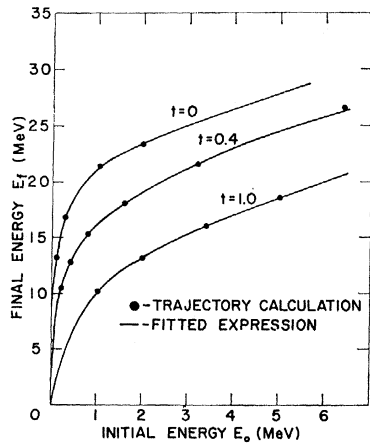


Fig. 8. Final kinetic energy  $E_f$  as a function of initial energy  $E_0$  and time, for  ${}^4\text{He}$  particles. Time is in units of  $10^{-21}$  sec.

released, and on the initial direction of motion of the third particle. In Fig. 8 we have taken the initial position as the potential minimum between the two fragments and the initial direction to be perpendicular to the interfragment axis. The final energy is approximately a minimum if the particle is released at the potential minimum and a maximum if the initial direction is perpendicular, as indicated in Fig. 9. For a fixed time and initial direction,  $A$  and  $B$  of Eq. (1) can be given quite accurately as

$$A = a + bz + cz^2, \quad B = d + ez + fz^2, \quad (2)$$

where  $z$  is the location of the third particle along the interfragment axis, and  $a$ - $f$  are empirical constants. If the parameters of Eqs. (1) and (2) are evaluated for an initial direction perpendicular to the interfragment axis, the dependence of  $E_f$  on initial angle can be expressed crudely by multiplying the result obtained from Eq. (1) by the quantity  $1 - (1 - \theta_0/90)^2$ , where  $\theta_0$  is

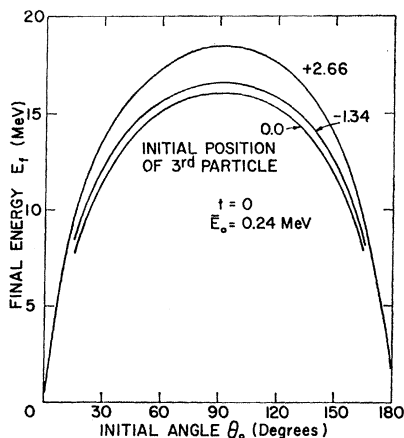


Fig. 9. Effect of initial position and initial direction on final kinetic energy for  ${}^4\text{He}$  particles. Distances are relative to the point of minimum potential between the two major fragments and are in units of  $10^{-13}$  cm.

the initial angle in degrees. The result will be correct at  $90^\circ$  and nearly correct at  $0^\circ$  and  $180^\circ$ .

Boneh, Fraenkel, and Nebenzahl<sup>13</sup> have shown that the dependence of final angle on initial angle is weak over the region of interest. In Fig. 10 the effect of initial position and energy on the final angle is shown. The fitted curves are obtained from the semiempirical equation

$$\theta_f = \alpha + \beta E_0 + z(\gamma e^{-\delta E_0} + \epsilon e^{-\eta E_0}), \quad (3)$$

where  $\theta_f$  is the final angle between the third particle and the light fragment and  $\alpha$ ,  $\beta$ ,  $\gamma$ ,  $\delta$ ,  $\epsilon$ , and  $\eta$  are empirical constants.

### Results of Monte Carlo Calculations and Comparison with Experimental Results

Using the model just described, it is now possible to see how successful such calculations are in accounting for the experimentally observed results. To do this it is first necessary to choose a reasonable and consistent set of input parameters. For this purpose, we have chosen to find a set that will reproduce the  ${}^4\text{He}$  energy spectrum. Such a choice is arbitrary of course, but is justified by several considerations. First, the energy spectrum is the most thoroughly studied and most well-defined feature of light-charged-particle emission. Second, each type of light particle has a characteristic energy spectrum (whereas, for example, the angular distributions are similar for all), thus providing the most sensitive test for the success of the calculations.

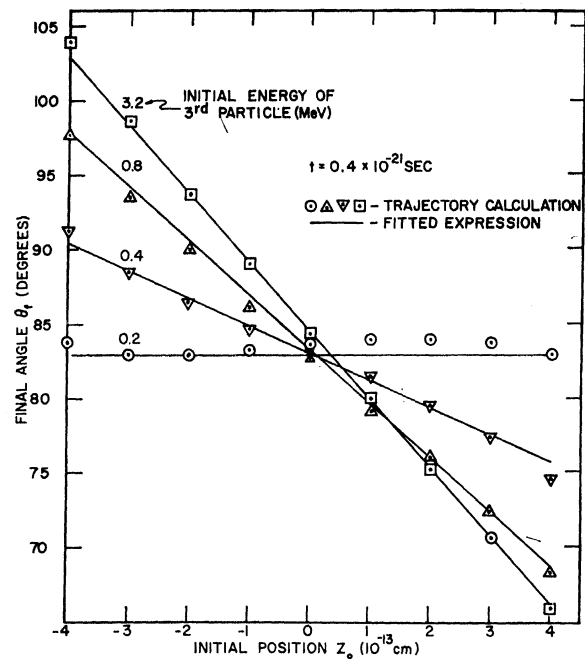


Fig. 10. Effect of initial position and initial energy on the final angle for  ${}^4\text{He}$  particles. The point of minimum potential between the fragments is  $Z = -0.76 \times 10^{-13}$  cm.

Finally, the calculated over-all energy spectrum is quite insensitive to the mass split assumed, and therefore the disadvantage of considering only the most probable division is minimized.

Since the final energy  $E_f$  is sensitive to both emission time and initial energy  $E_0$ , it was possible to find various pairs of these parameters that would give the measured  $^4\text{He}$  energy peak of 16 MeV. However, examination of the shape of the calculated spectra showed that the range of acceptable parameters was restricted considerably. If the choice of emission time was too short, the cutoff of the spectrum at the high end was too sharp, while if the time was too long, the  $\bar{E}_0$  necessary to maintain the peak gave too large a high-energy tail (Fig. 11). The best agreement is with  $t=0.4 \times 10^{-21}$  sec and  $\bar{E}_0$  about 2.0 MeV. These values seem physically reasonable, and it is interesting to note that their product is roughly equal to  $\hbar$ . Such a relationship might, at least naively, be expected on the basis of the uncertainty principle.

The above calculations were done with a distribution of initial positions along the interfragment axis characterized by a standard deviation of  $1.5 \times 10^{-13}$  cm. The final-energy spectrum is quite insensitive to this parameter.

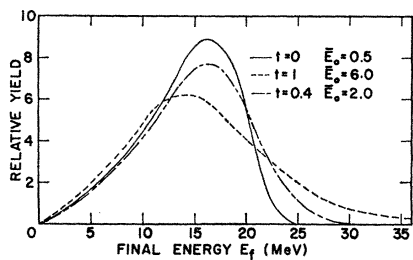


FIG. 11. Calculated energy spectra for  $^4\text{He}$ , using different assumptions about initial starting conditions. Units of  $t$  are in  $10^{-21}$  sec and for  $\bar{E}_0$  are in MeV.

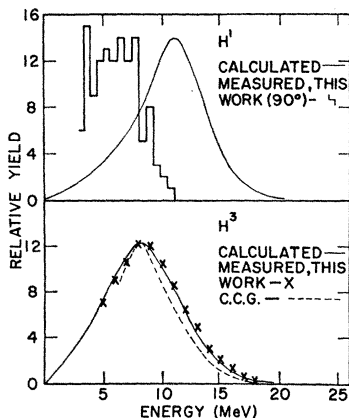


FIG. 12. Comparison of calculated and measured energy spectra for  $^1\text{H}$  and  $^3\text{H}$ . The experimental  $^1\text{H}$  data were obtained at  $90^\circ$ . The dashed line represents the data of Cosper, Cerny, and Gatti (Ref. 9).

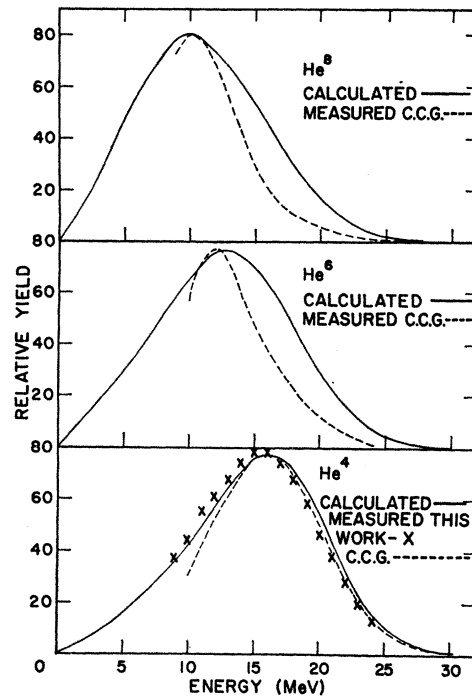


FIG. 13. Comparison of calculated and measured energy spectra for  $^4\text{He}$ ,  $^6\text{He}$ , and  $^8\text{He}$ . The dashed lines represent the data of Cosper, Cerny, and Gatti (Ref. 9).

Using the same set of parameters, which give a fit to the  $^4\text{He}$  spectra, we have calculated energy spectra for other particles. These are shown in Figs. 12-14. The

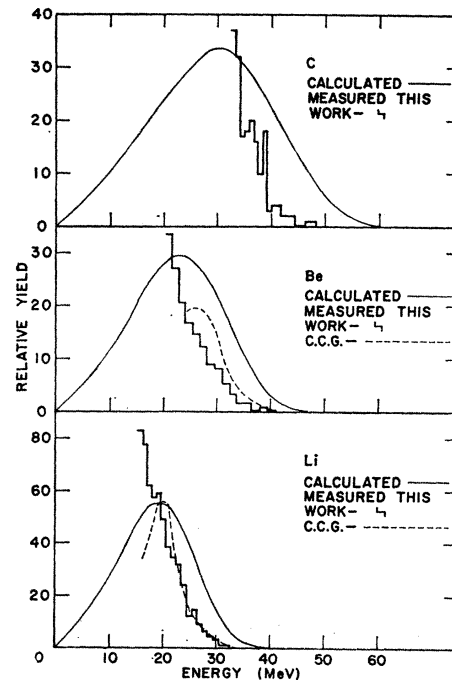


FIG. 14. Comparison of calculated and measured energy spectra for  $\text{Li}$ ,  $\text{Be}$ , and  $\text{C}$  ions. The dashed lines represent the data of Cosper, Cerny, and Gatti (Ref. 9).



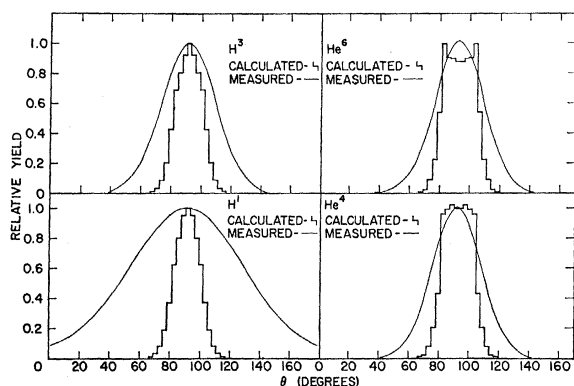


FIG. 15. Calculated and measured angular distributions for  $^1\text{H}$ ,  $^3\text{H}$ ,  $^4\text{He}$ , and  $^6\text{He}$ . The apparent separation of the calculated  $^6\text{He}$  peak into two parts is a result of events being associated with either the light or the heavy mass peak.

agreement with measured spectra is seen to be generally quite good, with the discrepancies becoming larger for the less abundant particles. The experimental data of Cospers, Cerny, and Gatti<sup>9</sup> have been used for comparison in most cases because they have the best statistical accuracy. Our data, in general, are in good agreement with theirs, except for lithium and beryllium as previously noted. In these two cases the calculated spectra seem to provide a peak roughly at the energy reported by them, but not found by us.

The one outstanding discrepancy between calculated and observed spectra occurs for the case of  $^1\text{H}$ . Because of the interferences of noncoincident protons, the overall spectra cannot be readily measured, but the comparison is shown in Fig. 12 for an angle of  $90^\circ$ . The disagreement is significant, especially in view of the rather excellent agreement for  $^3\text{H}$ . Possible explanations for this difference will be discussed later.

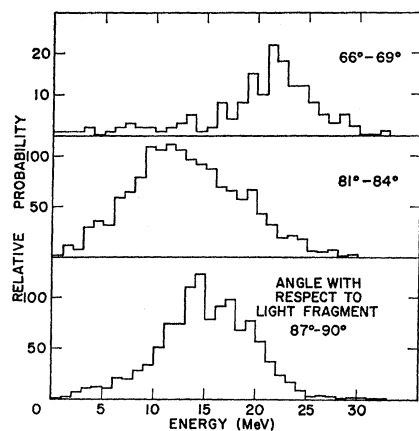


FIG. 16. Calculated energy spectra for  $^4\text{He}$  particles at various angles with respect to the light mass fragment. An initial distribution of positions corresponding to  $\sigma = 2.5 \times 10^{-13}$  cm was used in this calculation.

The second area in which we are interested involves the angular distribution of the various particles. Some of these distributions, calculated using the same set of parameters just described, are shown in Fig. 15. The characteristic peaking at  $90^\circ$  is clearly evident, and in general they are qualitatively in agreement with the experimental results. In making such a comparison it should be remembered that the measured distributions include some dispersion due to the angular resolution of the detectors and, more important, they are a composite of all possible mass divisions. In relation to the calculation, more symmetric divisions build up the peak near  $90^\circ$ , while very asymmetric divisions give rise to a tail in the distribution. Such effects are in the right direction to account for the present discrepancies between calculated and observed results.

An additional way to affect the final angular distribution is to start with a broader distribution about the initial starting position for the light particle. Such a change has a negligible effect on the energy calculations and, since the width parameter was chosen somewhat arbitrarily (at  $\sigma = 1.5$ ), would be entirely acceptable.

Once again, the obvious exception to the general agreement between calculation and experiment is noted for the protons. There is no indication in the calculated results that one should expect any broadening of the angular distribution for  $^1\text{H}$  in comparison with the others. It must be concluded, therefore, that the observed effect does indicate some real difference in the release conditions.

The third effect to be studied is the correlation between energy and angle of the third particle. Because the calculated distributions being used are somewhat narrower than those observed, this agreement is only qualitative, but clearly shows (Fig. 16) that the lowest-energy spectrum is observed for the most probable angle ( $81^\circ - 84^\circ$ ), with progressively higher-energy events being produced as one goes to smaller or larger angles. The reason for this is clear if one examines the starting conditions for individual events in the Monte Carlo routine. The most sensitive parameter in determining the final angle is the initial starting position. The majority of events are initiated from near the potential minimum, and are repelled more or less equally by both of the large fragments. There are, however, some particles that start near one of the fragments and initially are dominated by the large potential from that fragment. They tend to be projected away at an "off" angle, picking up greater than average energy in the process. It is these events that give rise to the hardening of the energy spectrum at the smaller (or larger) angles.

Another type of effect that can be noticed in studying the Monte Carlo results involves those relatively rare events (because of small solid angle) that are initially directed at one or the other of the large fragments. Such particles undergo a "rebound" effect, and as a result

suffer a significant decrease in their final energy. It is this type of event that gives rise to most of the lower-energy portion of the spectrum.

## V. DISCUSSION

The results presented seem to indicate fairly conclusively that all of the light fragments observed (with the possible exception of  $^1\text{H}$ ) are emitted by a similar mechanism. In this respect, so-called long-range  $\alpha$  fission should be considered as simply a specific example of a more general process. The energy spectra and angular distributions of these particles can be reasonably well explained by assuming that they are produced in the region between the large fragments shortly after scission, and are then accelerated by the Coulomb field of the separating fragments.

The low yield of these events is consistent with the fact that such a process would be expected to occur only in the rare instance when a relatively large amount of the scission energy is localized on a few nucleons, thus providing the necessary release energy. The general trend of decreasing yield with increasing charge supports this view. However, the fact that the beryllium yield appears to be as large as that of lithium and the carbon yield greater than that of boron (a certain amount of caution is necessary in making these estimates, since only a part of the total energy spectrum is observed) suggests that other factors (for example, pairing energy or clustering of the incipient light particle) may play a significant role.

The one feature of our results that does not seem to be readily accounted for by our model is the apparent anomalous behavior of the protons. The angular distribution and energy spectrum are inconsistent both with the characteristics of the other particles and with the calculations. Before discussing these differences, it is instructive to consider other possible sources of protons besides "scission" ones.

Although Cospers, Cerny, and Gatti<sup>9</sup> have shown that natural  $\alpha$  particles might be expected to give rise to a proton peak at about 5 MeV from  $(\alpha, p)$  reactions, our coincidence requirements preclude this as a source. Secondary  $(n, p)$  reactions could possibly contribute, since the prompt neutrons are effectively in coincidence with the fragments. However, because of the strong correlation between neutron and fragment direction, the secondary products would be expected to be peaked at  $0^\circ$  and  $180^\circ$ , rather than at  $90^\circ$  as observed. Similarly, one can discount the possibility of "knock-on" events induced by the large fragments, which would also show a positive correlation with fragment direction. Finally, one might consider protons evaporated from the excited fragments after scission. Calculations have been made to estimate the yield of such events,<sup>14</sup> and generally have predicted much lower abundance than observed.

Once again, if evaporation took place from the accelerated fragments, a correlation with fragment direction would result.

It would appear from the above considerations that none of the suggested sources could account, at least totally, for the coincident protons. Nevertheless, the possibility cannot be ruled out that they may provide a "background" of events which, because of the low abundance, could seriously distort the characteristics of the "scission" protons.

If one allows that the observed coincident protons are indeed "scission" events, produced in a similar environment to the other light particles, there remains the problem of accounting for their usual features. In discussing the relative yields of various light particles, Halpern<sup>2</sup> has made two points that might be relevant in the present context. The first is that nucleons, being less strongly absorbed in nuclear matter than more complex particles, could be expected to be released over a much larger volume, perhaps even one overlapping the larger fragments. This effective increase in the distribution of initial positions would indeed broaden the distribution of final angles.

The second point is that the protons, being relatively mobile, are less likely to experience a completely "sudden" snap at scission. There is, therefore, a greater chance that the protons that are released will have a lower initial energy. This in turn gives rise to a lower final energy.

A somewhat different approach is to consider the uncertainty principle again, this time with respect to the product of momentum and position uncertainty.

$$\Delta p \Delta z = \hbar.$$

If we associate the uncertainty in  $\Delta p$  with the initial energy  $E_0$ , we get

$$\Delta z = \hbar / (2mE_0)^{1/2}.$$

Assuming for the moment a constant  $E_0$ , it is clear that the smaller mass of the proton, as compared, say, to a  $^4\text{He}$ , will result in a much increased variance in  $z_0$ . For example, taking  $E_0$  as 2 MeV, we get

$$\Delta z(^4\text{He}) = 1.8 \times 10^{-13} \text{ cm},$$

$$\Delta z(^1\text{H}) = 3.6 \times 10^{-13} \text{ cm}.$$

This difference, in turn, will be reflected in a broader angular distribution for the protons. Thus it appears there may be several ways to account at least qualitatively for the differences in characteristics between the  $^1\text{H}$  and other light particles.

It may be of value at this point to compare some of our results and conclusions with those of Fraenkel *et al.*,<sup>5,13</sup> who have made a somewhat similar study for  $^4\text{He}$ . First of all, it should be noted that the agreement of the trajectory calculations is good, and no significant differences were apparent. The discrepancies in the parameters arrived at seem to result from slightly

<sup>14</sup> J. R. Grover and T. D. Thomas (unpublished results).

different approaches and some differences in experimental data. Our emission time of  $0.4 \times 10^{-21}$  sec (corresponding to a velocity of  $2.09 \times 10^8$  cm/sec for the heavy fragment and an interfragment distance of  $21.5 \times 10^{-13}$  cm) is somewhat earlier than that arrived at by them ( $1 \times 10^{-21}$  sec,  $4.4 \times 10^8$  cm/sec, and  $26 \times 10^{-13}$  cm, respectively). This difference arises in part because they fit their calculations to a significantly wider angular distribution than that found by us. The earlier release time means that the fragments have acquired a somewhat smaller portion of their final energy at release time than their work indicates. We have not found it necessary to postulate any correlation between  $E_0$  and  $\theta_0$ , primarily because our experimental correlation of  $E_f$  with  $\theta_f$  is stronger than theirs. Again, because of a narrower angular distribution, our variance ( $1.5 \times 10^{-13}$  cm) in initial starting positions is significantly smaller than theirs (about  $4 \times 10^{-13}$  cm).

No serious issue should be made over the differences between our parameters and those derived by Fraenkel *et al.*<sup>13</sup> Our goal has been to see if this model with a single set of parameters could account for the energy spectra of the various light particles. Theirs was to find a set of parameters that could account for more detailed data on  $\alpha$ -particle emission. Further work would be needed to see if some compromise between their assumptions and ours might fit all of the results satisfactorily.

It is interesting to speculate on the possible relationship of the light-charged-particle (LCP) tripartition considered here, and the more controversial "ternary fission," in which all three fragments are of comparable size. (Although both have been referred to as ternary fission, we would prefer to reserve the term for the latter phenomenon.) From all the evidence so far, it would appear reasonable to assume that even heavier "light" particles are emitted by the mechanism considered here. On the other hand, the probability of localizing sufficient release energy for such particles would be expected to make their abundance extremely small.

Some reports on ternary fission<sup>15,16</sup> have suggested a yield of the order of 1 in  $10^6$  fissions, which is much larger than would be expected on the basis of the trend of the LCP results. However, it has also been suggested<sup>16</sup> that at least part of these ternary events may consist of a relatively small fragment (i.e., mass less than 30) accompanied by two larger fragments. A preference for such divisions appears to be indicated by studies at higher excitation energies.<sup>17</sup> An interesting question, therefore, is whether such products (if they exist) are simply an extension of the LCP mechanism, or whether they represent a fundamentally different type of fission. Trajectory calculations of the type discussed here have been made for heavier particles and indicate that, even at mass 25, the LCP would be expected to be rather strongly correlated at roughly  $90^\circ$  with respect to the larger fragments. On the other hand, much of the emphasis on ternary fission has been directed at looking for a substantially different process; that is, one which would lead to the fragments coming apart at about  $120^\circ$  to each other.<sup>15,16</sup> Such a distinguishing characteristic may prove useful in exploring and classifying the two processes.

#### ACKNOWLEDGMENTS

The californium from which the source was prepared was lent to us by the Division of Research of the U. S. Atomic Energy Commission. The original material was prepared by Robert Latimer of the Lawrence Radiation Laboratory, to whom we are grateful. We would like to thank Tom Madden of Bell Telephone Laboratories for making the very thin detectors used, and John Lehman for programming the trajectory calculations.

<sup>15</sup> M. L. Muga, in *Proceedings of the Symposium on Physics and Chemistry of Fission* (International Atomic Energy Agency, Vienna, 1965), Vol. II, p. 409.

<sup>16</sup> M. L. Muga, C. R. Rice, and W. A. Sedlacek, *Phys. Rev.* **161**, 1266 (1967).

<sup>17</sup> R. H. Iyer and J. W. Cobble, *Phys. Rev. Letters* **17**, 541 (1966); and (to be published).

---

## Erratum

---

**Generalized Hartree-Fock Approximation for Nucleon-Nucleon Scattering**, LOUIS CELENZA [Phys. Rev. **168**, 1189 (1968)]. The title should read, "Generalized Hartree-Fock Approximation for Nucleon-Nucleus Scattering." In Eq. (43) the last prime should be within brackets. The sentence containing Eq. (58) should contain a reference to Eq. (55) rather than to (56).